Effects of different moisture contents on the structure and properties of corn starch during extrusion

Bin Wang [a,b], Yuqing Dong [a,b], Youxin Fang [c], Wei Gao [a,b], Xuemin Kang [a,b], Pengfei Liu [a,b], Shouxin Yan [a,b], Bo Cui [a,b,*], A.M. Abd El-Aty [b,d,e,*]

[a] School of Food Science and Engineering, Qilu University of Technology, Shandong Academy of Sciences, Jinan, Shandong 250353, China
[b] State Key Laboratory of Biobased Material and Green Papermaking, Qilu University of Technology, Shandong Academy of Sciences, Jinan 250353, China
[c] Department of Forestry College, Shandong Agricultural University, Taian 271018, China
[d] Department of Pharmacology, Faculty of Veterinary Medicine, Cairo University, 12211 Giza, Egypt
[e] Department of Medical Pharmacology, Medical Faculty, Ataturk University, Erzurum, Turkey

ARTICLE INFO

ABSTRACT

Herein, corn starch samples with different moisture contents (native corn starch, 30, 35, 40, 45, and 50%) were prepared by twin-screw extrusion, and the structural and physical properties were analyzed and correlated. Scanning electron microscopy observed the morphology, attenuated total reflection-Fourier transform infrared spectroscopy investigated the double helix structure, X-ray diffraction analyzed the crystal region, ion chromatography observed the chain length distribution, and rapid viscosity analyzer measured the viscosity of corn starch samples. We found that the corn starch crystallinity, degree of order, and double helix degree decreased with increasing moisture content. The moisture content has a crucial role in the peak viscosity, breakdown, final viscosity, and setback in pasting property experiments. With the increase in moisture content, the longer chain was transformed into a shorter chain, and the dispersion of molecular weight distribution continuously increased. This study provides a theoretical basis for the production of extruded corn starch.

1. Introduction

Starch is a primary carbohydrate source in the human diet (Zhang, Hu, Zhu, Wu, & Tan, 2018). It is a complex carbohydrate composed of amylose and amylopectin (Wang et al., 2021), widely used in food production. Among different types of starch, corn starch is the focus of current research due to its low price and excellent physical and chemical properties (Wang et al., 2021). However, because of the corn starch's inherent shortcomings, it is needed to mix it with other materials to achieve the best performance (Wang et al., 2021). The hydrophobicity and solubility of corn starch are poor (Cai et al., 2019). There are many ways to treat starch, such as hydrothermal treatment (Yu, Ma, & Sun, 2009), annealing, heat treatment, high hydrostatic pressure treatment (Hu et al., 2011), ultrasound (Jiang et al., 2011), and extrusion. It has to be noted that the hydrothermal and heat treatments require lower temperatures, and the extent of starch gelatinization is low. In contrast, high hydrostatic pressure and ultrasonic treatment are not very mature.

Extrusion treatment is a high-temperature short-time food processing technique, which is now considered a mature manufacturing process (Li, Hasjim, Xie, Halley, & Gilbert, 2014). The physicochemical properties of extrudates were dependent on the high temperature, pressure, and high shear force (Singh, Gamlath, & Wakeling, 2007). The extrusion process can physically modify starch to obtain expandable starch products, snacks, and cornflakes (Singh et al., 2007). Simultaneously, starch products have specific texture and sensory properties (Singh et al., 2007). Generally, extrusion can lead to corn starch gelatinization, the disappearance of crystallinity, and degradation of amylose and amylopectin under low moisture content (Chiu & Solarek, 2009). Food extrusion technology is widely used to produce textured protein, expanded food, protein modification, and starch modification. In this context, Garcia-Valle, Agama-Acevedo, Nuñez-Santiago, Alvarez-Ramirez, and Bello-Pérez (2021) have evaluated the *in vitro* effects of starch, protein, and fat content (in flour) on the viscoelasticity and starch digestibility of mango powder and amaranth powder. They found that extrusion led to gelatinization of starch in amaranth and mango powder, destroyed the long-range and short-range ordered starch

---

structure, and increased the content of slowly digested starch in amaranth powder. Further, Zhang et al. (2020) investigated the changes in structural and functional properties of starch-based polymers in barley flour during low moisture extrusion. They found that extrusion significantly reduced ($P < 0.05$) the contents of starch, protein, fiber, and fat in barley flour after extrusion. The color of barley flour darkened, indicating Maillard reaction and caramelization reaction. Moreover, various cracks, pits, and holes have appeared on the surface of extruded barley flour. Extrusion leads to molecular degradation of starch and reduces its swelling power in water, and the extrudate still has Δ H (0.19–0.71 J/g), indicating that starch is not completely gelatinized. Further to that, Téllez-Morales, Herman-Lara, Gómez-Aldapa, and Rodríguez-Miranda (2020) simulated the interaction between starch and protein in food system through single screw extrusion of corn starch and whey protein isolate blends. Additionally, Yan et al. (2019) used an extrusion-heat-moisture combination to treat corn starch to explore the physicochemical properties and digestibility of corn starch. They showed that extrusion played a leading role in reducing the relative crystallinity and resistant starch content of corn starch. The swelling power, solubility and digestibility of corn starch increased after extrusion. (Wani, Farooq, Qadir, & Wani, 2019) extruded Bangladesh chickpea starch for a short time at a high temperature. They found that the extrusion significantly reduced the content of amylose, darkened the color of the sample, increased its solubility, and decreased its gelatinization properties.

Moisture content is an important factor in extrusion and can affect the gelatinization degree, crystallinity, amylose and amylopectin degradation of corn starch (Liu et al., 2019). Therefore, this study used corn starch as a raw material to investigate the effect of different moisture contents on corn starch during extrusion. Herein, corn starch was used as raw material, and different proportions of distilled water (30, 35, 40, 45, and 50%, starch dry weight basis) were added. After that, the samples were prepared by a twin-screw extruder to assess the micromorphology, crystallinity, amylose and amylopectin changes of as-prepared starch. The molecular structure, long-range ordered structure (crystalline structure), short-range ordered structure, and particle morphology were characterized by modern detection technology. The changes of physical and chemical properties before and after extrusion were also analyzed.

2. Materials and methods

2.1. Materials

Commercial corn starch (with amylose content of 33.81% and amylopectin content of 66.19%) was purchased from Xiangchi Corporation (Boxing, Shandong, China). Absolute ethanol, dimethyl sulfoxide (chromatographic purity), sodium nitrate, dimethyl sulfoxide-D6, sodium acetate $\geq$ 99.0% and glacial acetic acid were acquired from Sigma Co., Ltd. (St. Louis, MO, USA). Isoamylase was secured from Shanghai Anpu Experimental Technology Co., Ltd. (Shanghai, China).

2.2. Preparation of corn starch samples by extrusion

In this experiment, a co-rotating twin-screw extruder (SHJ20, Nanjing giant Machinery Co., Ltd, Nanjing, China) was used. The ratio of length to the diameter of the extruder is L/D $\approx$ 40, and the maximum temperature and screw speed are 300 ℃ and 600 rpm, respectively. The barrel temperatures for zone 1, 2, and 3 were kept at 70, 90, and 100 ℃. Corn starch and water of different proportions (starch dry weight basis, 30, 35, 40, 45, and 50%) were premixed in a blender for 10 min to obtain corn starch with moisture contents of 30, 35, 40, 45, and 50%. After that, the corn starch sample was sealed in a polyethylene self-sealing bag, stored at 25 ℃ for 48 h for equilibration and uniform distribution of corn starch and moisture. In the extrusion process, the corn starch sample was fed into the hopper at a feed speed of 10 *Hz*, and the main

engine speed of the extruder was adjusted to 15 *Hz*. The corn starch sample was passed through a heating bucket of 850 mm, and then the sample was extruded from the barrel of a single nozzle with a diameter of 22 mm. After the extrusion was completed, the corn starch sample was air-dried at 25℃ for 24 h, and then the steady-state sample was ground and passed through a 100-mesh powder for further analysis.

2.3. Water absorption

The water absorption of corn starch samples was determined according to the method described by Yu, Liu, Tang, Shen, & Liu (2017). The weighing bottle was washed and dried in an oven at 105℃ to a constant weight. Afterward, 2.5 g sample was evenly mixed with 30 mL deionized water, stirred in a water bath for 30 min at 30℃, centrifuged at 6000 rpm for 10 min, and then the supernatant was removed. The residue was dried at 60℃ to a constant weight, and the water absorption was calculated as follows.

$$WAI = \frac{M_2 - M_1}{M_2} \times 100\%$$

where M_1 is the precipitation mass after drying, M_2 is the precipitation mass after centrifugation; the unit is g.

2.4. Scanning electron microscopy (SEM)

Corn starch samples were observed by scanning electron microscopy (SEM, Hitachi SU3500, Tokyo, Japan) under an accelerated voltage of 5 kV (Arribas, Cabellos, Cuadrado, Guillamón, & Pedrosa, 2019). The sample was spread on double-sided carbon-coated tape and gold-plated on the installed sample. Then, the microstructure of the corn starch was photographed by an SEM (Scan factor: 400).

2.5. X-ray diffraction (XRD)

The corn starch sample was ground into powder (200-mesh) and then scanned with an X-ray diffraction (XRD, IV X-ray diffractometer, Tokyo, Japan) instrument to obtain the XRD map (Liu et al., 2021). A special glass sheet was used to prepare corn starch samples for further XRD analysis. Diffractograms were collected at 40 kV and 30 mA with nickel-filtered Cu-Kα radiation (wavelength 1.5405) (Xu, Chen, Luo, & Lu, 2019). The scanning range of the sample was ranged between 3°~ 35°, and the scanning rate was 4°/θ (Xu et al., 2019). Each corn starch sample was scanned at least three times. The XRD patterns of corn starch samples were analyzed by Jade 5.0 software (Materials Data Inc., California, USA).

2.6. ATR-FTIR spectroscopy analysis

Corn starch samples with different moisture contents were evaluated by attenuated total reflection-Fourier transform infrared spectroscopy (ATR-FTIR, Bruker, V70FTIR, Berlin, Germany) as described elsewhere (Liu et al., 2020; von Borries-Medrano, Jaime-Fonseca, Aguilar-Méndez, & García-Cruz, 2018). Samples were uniformly spread on the surface of diamond ATR crystal, and the air background was scanned and recorded. An ATR-FTIR was scanned 32 times with a resolution of 0.16 cm^{-1}, and the wavenumber range was 800–3500 cm^{-1}. The final scanning results were assessed in detail by PeakFit. The infrared absorptivities at 1047/1015 cm^{-1} (DO) and 995/1015 cm^{-1} (DD) were further examined.

2.7. Pasting properties

The peak viscosity (PV), trough viscosity (TV), disintegration viscosity (BD), final viscosity (FV), and setback (ST) of corn starch samples with different moisture contents were measured by a rapid viscosity

analyzer (RVA, RVA-TM, Perten, Swedish) as described by Dos Santos et al. (2018). First, 3 g corn starch samples were weighed and then mixed with 25 mL distilled water. The rotational speed of the plastic pulp was 960 rpm in the first 10 s and 160 rpm in the fertility test. The sample was kept at 35℃ for 1 min, heated to 90℃ at a rate of 10℃/min, kept at 90℃ for 3 min, and cooled to 35℃ at a rate of 10℃/min.

2.8. Molecular-weight distribution

In this experiment, a gel chromatography-differential-multi-angle laser light scattering system was used. The differential detector is an Optilab *T*-rEX laser light scattering detector (Wyatt Technology, CA, USA) (Gong, Cheng, Gilbert, & Li, 2019). According to the properties of the compound, the gel exclusion chromatographic columns of Ohpak SB-805 HQ (300 × 8 mm, Wyatt Technology, CA, USA), Ohpak SB-804 HQ (300 × 8 mm, Wyatt Technology, CA, USA), Ohpak SB-803 HQ (300 × 8 mm, Wyatt Technology, CA, USA), and column temperature of 60℃ were used for DAWN HELEOS II (Wyatt Technology, CA, USA). The injection volume was 100 μL, and the mobile phase of 0.1 m NaNO$_3$ was used. Five milligrams of the starch sample were dissolved overnight in 1 mL DMSO by heating in a 100℃ water bath. Subsequently, 3 mL anhydrous ethanol was added into the solution and then centrifuged (5000 rpm, 15 min) to remove the supernatant. The collected sediment was washed twice with anhydrous ethanol. After that, it was dissolved in 3 mL 0.1 M NaNO$_3$ and centrifuged at 12000 rpm for 10 min. Finally, 100 μL was filtered (0.45 μm organic filter membrane, Shanghai Anpu
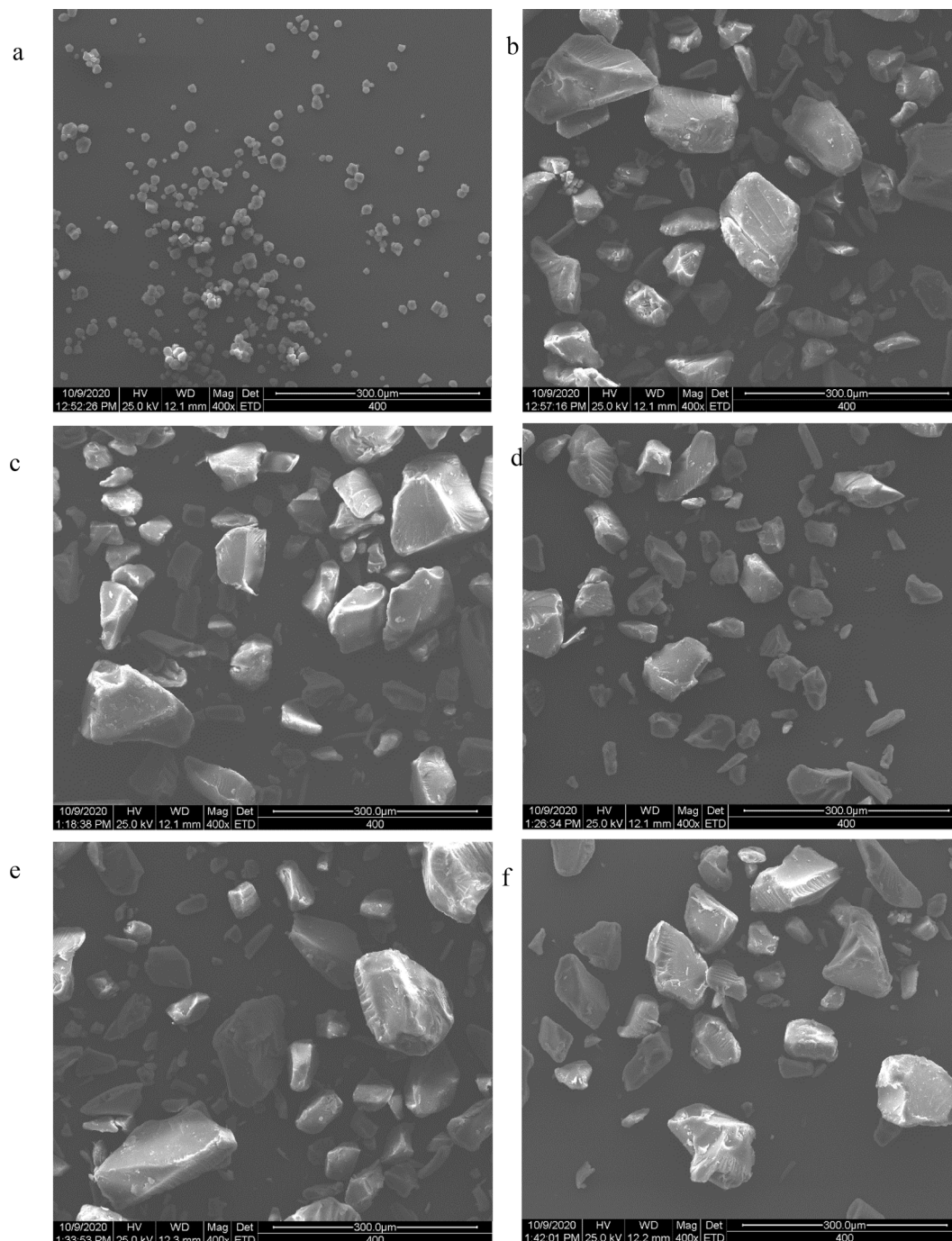
Fig. 1. Scanning electron microscopic images of corn starch: (a) native corn starch, (b) 30%, (c) 35%, (d) 40%, (e) 45%, and (f) 50%.

Experimental Technology Co., Ltd. Shanghai, China) before injection.

2.9. Chain length distribution

Ion chromatography (Wyatt Technology, CA, USA) was used to detect the chain length distribution of corn starch samples (Li et al., 2020; Wu, Li, & Gilbert, 2014). First, 10 mg sample was dissolved in 3 mL 90% DMSO by heating and stirring in a boiling water bath for 20 min. Then, 10 mL anhydrous ethanol was added to the suspension, the suspension was centrifuged at 5000 rpm for 15 min, and the residue was removed. The residue was dissolved in 3 mL 40 mmol/L (pH = 4) sodium acetate buffer solution by heating and stirring in a boiling water bath for 25 min. Ten microliters of isoamylase were added to the solution and debranched at 40 ℃ for 24 h. The solution was kept in a boiling water bath for 20 min to stop the debranching reaction. Next, 1 mL sample was dissolved in 3 mL 150 mmol/L NaOH. Finally, the sample was filtered by a 0.45 μm filter membrane (Shanghai Anpu Experimental Technology Co., Ltd. Shanghai, China) and injected onto ion chromatography.

2.10. Statistical analyses

The mean and standard deviation of three repeated measurements were analyzed using SPSS 19 statistical software (version 13.0, Statistical Package for the Social Sciences Inc., Chicago, USA). The significant differences were analyzed by factor analysis of variance and Tukey correction at $P < 0.05$.

3. Results and discussion

3.1. SEM

The granular structure of corn starch was observed by electron microscopy. The native corn starch granules were polygonal, and the edges were relatively smooth with a small number of stomata, as shown in Fig. 1. After extrusion, the granules were destroyed due to the thermal effect and shear force replaced by a rougher, irregular, and broken structure. Fig. 1 shows that the moisture content has little effect on the extruded corn starch, and there was no obvious difference in each group of corn starch samples. In this context, L. Wang, Shogren, and Willett (1997) found that the extruder's high temperature and high shear force would destroy the starch structure during extrusion. Further, Wang et al. (2021) stated that starch gelatinization was affected by temperature, and there was no gelatinization reaction at a temperature range of 50-60℃. Gelatinization occurs when starch granules are heated between 70 and 80℃. Under this condition and in the presence of water, the particles expanded and melted and finally disintegrated and formed uniform gels.

3.2. Water absorption

Water absorption reflects the water holding capacity of the corn starch samples, which is an indirect determination for intact starch granules and fully gelatinized starches. It can be used as an index of starch integrity in gelatinization and a water dispersion system (Yu, Liu, Tang, Shen, & Liu, 2017). As shown in Table 1, the water absorption of extruded corn starch was significantly increased compared with native corn starch. This finding indicates that the gelatinization reaction of corn starch occurs during extrusion. With the increase of water content, the gelatinization extent of corn starch increased, denoting that water would affect the gelatinization reaction of corn starch (Wang et al., 2021). These results might be attributed to variation in the degree of starch gelatinization during extrusion, which causes swelling and rupture of particles and exudation of amylose, leading to disruption of the intermolecular and intramolecular hydrogen bonds, and finally, destruction of crystal structure. After that, more hydrogen is exposed to

Table 1
XRD analysis, water absorption, and ATR-FTIR spectroscopy of corn starch with different moisture contents (native corn starch, 30, 35, 40, 45, and 50%).

Sample (%)	Relative crystallinity (%)	Water absorption index (%)	Degree of order (1047/1015)	Double helix degree (995/1015)
Native corn starch	20.54 ± 0.65^a	0.37 ± 0.08^e	1.45 ± 0.01^a	0.95 ± 0.03^a
30	10.27 ± 0.12^b	8.16 ± 0.45^d	1.38 ± 0.05^{ab}	0.94 ± 0.02^a
35	9.18 ± 0.48^c	10.45 ± 0.30^{cd}	1.36 ± 0.02^b	0.90 ± 0.05^{ab}
40	9.10 ± 0.49^c	12.97 ± 1.84^{bc}	1.34 ± 0.02^b	0.86 ± 0.03^{abc}
45	7.57 ± 0.04^d	14.64 ± 1.67^{ab}	1.33 ± 0.03^b	0.83 ± 0.02^{bc}
50	4.27 ± 0.10^e	17.32 ± 2.19^a	1.30 ± 0.03^b	0.79 ± 0.03^c

Data are presented as the X ± SD, different superscript letters in the same column denote significant differences (Duncan's range test, $P < 0.05$).

form hydrogen bonding with water, which increases the water absorption of extruded corn starch samples. The higher the degree of gelatinization, the greater the water absorption. Wang et al. (2021) stated that the gelatinization reaction of corn starch gradually occurs with the increase of temperature, which leads to a series of events, such as fragmentation of corn starch particles, destruction of chain structure, and destruction of crystal region.

3.3. XRD

The X-ray diffraction patterns of native starch and corn starch with different moisture contents are shown in Fig. 2. Corn starch has characteristic peaks at 15°, 17°, 18°, and 23°, which indicate type A crystallization. In this context, Fitch-Vargas et al. (2016) found that corn starch belongs to an A-type crystal structure. From Table 1, the crystallization zone of extruded corn starch almost disappeared compared with the raw material. We infer that the crystal region of corn starch was destroyed after high temperature and high shear force in the process of extrusion (Fitch-Vargas et al., 2016). With increasing moisture content, the crystallinity of corn starch decreases gradually. The higher the water content in the raw material of corn starch, the easier the absorption of water by starch particles and the faster the granules expansion. Thus, corn starch with high moisture content was easier to gelatinize, and the crystallinity decreases with increasing moisture content (Koa, Jin, Zhang, & Sopade, 2017). The characteristic peak of corn starch was not found at 2 θ = 20°. However, after extrusion, the characteristic peak of corn starch was found at 2 θ = 20°, and we inferred that the peak was
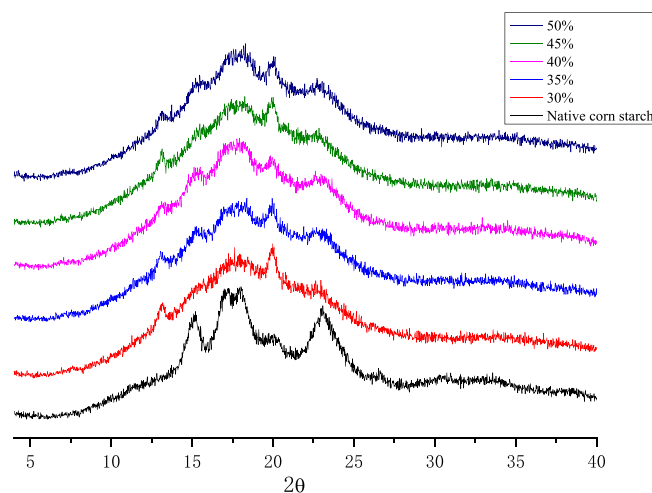
Fig. 2. X-ray diffraction of corn starch with different moisture contents (native corn starch, 30, 35, 40, 45, and 50%).

associated with V-type. The V-type crystal peak indicates that corn starch forms an amylose–lipid complex during extrusion (Wang et al., 2021). The study of Fitch-Vargas et al. (2016) showed that cereal starch could form amylose–lipid complexes by extrusion, and the crystal form is V-type.

3.4. ATR-FTIR

The short-range ordered structure of corn starch can be observed by ATR-FTIR, especially changes in the double helix structure (Yin, Ma, Hu, Li, & Boye, 2018). Fig. 3 shows the deconvolution spectra of raw materials and corn starches with different moisture contents after extrusion. From 1200 cm^{-1} to 800 cm^{-1}, we think most of them result from C—O and C—C stretching vibrations. This range was very sensitive to the physical state of corn starch (Bello-Pérez, Ottenhof, Agama-Acevedo, & Farhat, 2005). The 1047 cm^{-1} and 1016 cm^{-1} spectra represent the change sensitivity of the corn starch crystal structure and amorphous region, respectively (Capron, Robert, Colonna, Brogly, & Planchot, 2007). Similarly, 995 cm^{-1} represents the stretching vibrations of C—O - C and C—O - H (van Soest, Tournois, de Wit, & Vliegenthart, 1995). Our experiment focused on 1047/1015 cm^{-1} in the degree of order (DO) and 995/1015 cm^{-1} in the double helix (DD) of the corn starch crystalline region (Liu, Wang, Liao, & Shen, 2020).

With increasing moisture content, the values of DD and DO decrease gradually, as shown in Table 1. The value of DO decreased from 1.45 to 1.30, and the value of DD decreased from 0.95 to 0.79. As mentioned above, the gelatinization degree of corn starch increases with increasing moisture content. The corn starch gelatinization was accompanied by the destruction of the crystal region, mainly composed of amylopectin, whereas amylopectin has a double helix structure. In turn, we may conclude that the higher the gelatinization degree of corn starch is, the greater the destruction of the double helix structure of amylopectin. As a result, DD and DO decreased gradually with the increasing moisture content of corn starch. In this context, Wang et al. (2021) proved that the gelatinization process of starch was accompanied by the destruction of the crystal structure and the dissociation of the amylopectin double helix. During extrusion, the moisture content affects the gelatinization degree of starch, and the higher the moisture content, the higher the gelatinization degree of starch.

3.5. Pasting properties

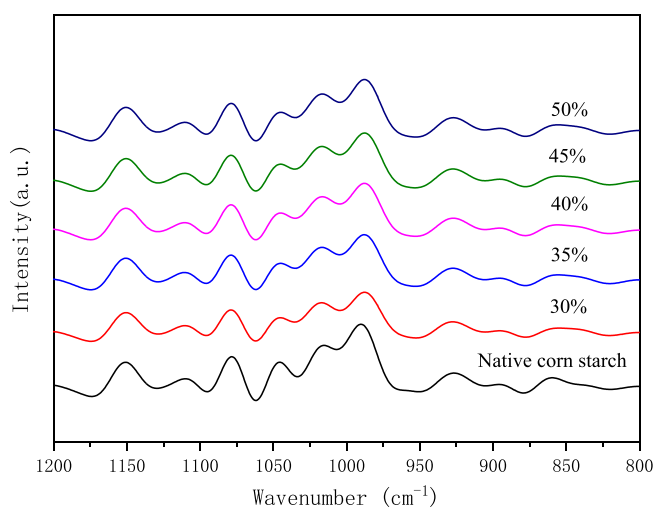The gelatinization characteristics of materials and corn starch with

Fig. 3. Attenuated total reflection-Fourier transform infrared spectroscopy of corn starch with different moisture contents (native corn starch, 30, 35, 40, 45, and 50%).

different moisture contents after extrusion are shown in Table 2. The peak viscosity, trough viscosity, and final viscosity of corn starch were 2.819, 1.891 and 3.740, respectively. We found that the viscosity of corn starch with different moisture contents decreased with increasing moisture content after extrusion.

According to a previous report, the peak viscosity (PV) was considered the equilibrium point between the expansion and fragmentation of starch particles (Zaidul, Norulaini, Omar, Yamauchi, & Noda, 2007). The swelling degree becomes low, resulting in a decrease in PV in the RVA experiment. According to Table 2, with increasing moisture content, the PV of corn starch decreases. We may imply that the gelatinization degree of corn starch increased with the increase of water content, so intact or residual starch granules decreased with water content. In turn, less water is absorbed in the RVA experiment; hence the PV was decreased. In this context, Zaidul et al. (2007) reported a negative correlation between peak viscosity and amylose content. Starch gelatinization can destroy the chain-like structure of corn starch. In this chain length distribution experiment, we proved that the transformation of corn starch samples from the longer chain (B1 ~ B2) to the shorter chain (A). Because the degree of gelatinization increases with the increase of water content, the peak viscosity of corn starch decreases with the decrease of water content. Further, BeMiller (2011) proved that fewer starch particles absorb less water in the RVA experiment, resulting in a decrease in PV.

Table 2 shows that breakdown (BD) increased with increasing moisture content, and there was a significant difference among groups ($P < 0.05$). In general, BD is the gel stability of starch (Liu et al., 2016). The experimental results showed that the gel stability of corn starch was higher with increasing moisture content. We believe that the final viscosity (FV) was related to the dissociation of amylose molecules and short-term regeneration during cooling. The difference in value between TV and FV was setback (ST). The experimental data showed that FV and ST decrease with increasing moisture content. We may speculate that the extrusion process has an important effect on the short-term retrogradation of corn starch. Liu et al. (2016) showed that extruded corn starch has higher water retention, thus delaying the retrogradation of corn starch.

3.6. Molecular-weight distribution

The Mw (weight-average molecular weight), Mn (number-average molecular weight), and Mw/Mn (D) (the degree of dispersion of the molecular weight distribution) of raw materials and extruded corn starch with different moisture contents are listed in Table 3. In Mw/Mn (D), D = 1 corresponds to a polymer with uniform molecular weight. The

Table 2
Pasting properties of corn starch with different moisture contents (native corn starch, 30, 35, 40, 45, and 50%).

Sample (%)	Peak viscosity (Pa·s)	Trough viscosity (Pa·s)	Breakdown (Pa·s)	Final viscosity (Pa·s)	Setback (Pa·s)
Native corn starch	2.819 ± 0.020[a]	1.891 ± 0.010[a]	0.928 ± 0.014[a]	3.740 ± 0.029[a]	1.849 ± 0.034[a]
30	0.675 ± 0.005[b]	0.385 ± 0.004[b]	0.290 ± 0.008[b]	0.650 ± 0.007[b]	0.265 ± 0.006[a]
35	0.649 ± 0.007[c]	0.348 ± 0.003[c]	0.302 ± 0.008[b]	0.620 ± 0.002[c]	0.272 ± 0.003[a]
40	0.634 ± 0.018[c]	0.313 ± 0.008[d]	0.321 ± 0.011[c]	0.570 ± 0.020[d]	0.257 ± 0.013[a]
45	0.625 ± 0.012[d]	0.264 ± 0.002[e]	0.361 ± 0.013[d]	0.519 ± 0.004[e]	0.256 ± 0.005[b]
50	0.601 ± 0.058[e]	0.224 ± 0.002[f]	0.386 ± 0.001[e]	0.476 ± 0.008[f]	0.253 ± 0.006[c]

Data are presented as the X ± SD, different superscript letters in the same column denote significant differences (Duncan's range test, $P < 0.05$).

Table 3
Starch chain length distribution and molecular-weight distribution of corn starch with different moisture contents (native corn starch, 30, 35, 40, 45, and 50%).

Samples (%)	A (DP 6–12)	B1 (DP 13–24)	B2 (DP 25–36)	B3 (DP ≥ 37)	M_w (×10^3 g/mol)	M_n (×10^3 g/mol)	M_w/M_n
Native corn starch	26.01[e]	55.24[a]	14.18[a]	4.58[c]	26530.7[a]	9145.9[a]	2.901[a]
30	27.06[d]	54.72[a]	13.70[b]	4.53[c]	9694.7[b]	3372.1[b]	2.875[a]
35	27.75[c]	54.16[a]	13.32[c]	4.79[a]	9533.9[b]	3087.4[bc]	3.088[a]
40	27.91[b]	54.28[a]	13.13[e]	4.68[b]	9016.6[bc]	2898.3[c]	3.111[a]
45	27.87[b]	54.03[a]	13.35[c]	4.75[a]	8633.9[bc]	2684.7[c]	3.216[a]
50	28.13[a]	53.84[a]	13.26[d]	4.77[a]	7463.7[c]	2252.9[d]	3.313[a]

Data are presented as the X ± SD, different superscript letters in the same column denote significant differences (Duncan's range test, $P < 0.05$).

higher the value of D, the wider the molecular weight distribution and the greater the polydispersity. The D value of corn starch was higher than that of extruded corn starch with different moisture contents, indicating that the double helix dissociation of amylopectin and the stripping of amylose during gelatinization are caused by the influence of high temperature and shear force during extrusion (Table 3). This phenomenon finally leads to a change in the molecular weight of corn starch. The D value increases with increasing moisture content. It is assumed that moisture content affects the gelatinization of corn starch. The gelatinization process of corn starch was often accompanied by the dissociation of amylopectin double helix and the dissociation of amylose. With increasing moisture content, the gelatinization degree of corn starch also deepens. Therefore, with increasing gelatinization degree, the double helix dissociation degree of amylopectin and the free degree of amylose also deepen. Finally, the D value increases with increasing moisture content. In this context, Gomez and Aguilera (1984) concluded that starch leads to amylopectin helical dissociation and amylose dissociation in the process of gelatinization. Further, Fitch-Vargas et al. (2016) found that the gelatinization degree of starch during extrusion was positively correlated with the moisture content in starch. In addition, amylose and amylopectin in starch are degraded due to high shear force and high temperature in the extrusion process (Moad, 2011).

3.7. Starch chain length distribution

According to the amylopectin cluster model, corn starch was divided into four chain lengths: A (DP 6–12), B1 (DP 13–24), B2 (DP 25–36), and B3 (DP ≥ 37) (C. Li & Gong, 2020). Amylopectin short chains include A (DP 6–12) and B1 (DP 13–24) chains, forming a double helix and the main components of the crystal region of corn starch particles. As seen in Table 3, the chain lengths of the four chains of corn starch raw materials are 26.01, 55.24, 14.18, and 4.58. With increasing moisture content, the number of A chains increased, whereas the number of B1 and B2 chains decreased. At high temperatures and high shear stress, longer B1 and B2 chains are degraded into shorter A chains. In addition, the gelatinization degree of corn starch under various moisture contents was altered after extrusion. The gelatinization essence of corn starch is the double helix dissociation. The destruction of amylopectin leads to a decrease in long chains B1 and B2 and an increase in the A chain in corn starch (Li & Gong, 2020). Generally, the longer the internal chain of amylopectin is, the greater the flexibility of the double helix of amylopectin, and the starch has a more stable crystal structure (Li & Gong, 2020).

4. Conclusion

Herein, corn starch samples were prepared by twin-screw extrusion, and the effect of water content on the structure and properties of corn starch was evaluated. We found that water content had a crucial impact on corn starch gelatinization. The gelatinization degree increased with increased moisture content, and the crystallinity, degree of order, and double helix degree of corn starch samples decreased. Further, moisture content has an important impact on peak viscosity, breakdown, final viscosity, and setback. With the increase of water content, molecular weight distribution was increased, which changed the long branched-chain to a short-chain. The chain structure of corn starch with

different water content was destroyed after extrusion, and the degree of damage deepened with the increase of water content. This study provides a possibility for the molecular mechanism of the change of water content of corn starch during puffing. It provides a theoretical basis for the production of extruded corn starch.

CRediT authorship contribution statement

Bin Wang: Investigation, Software, Visualization, Writing - original draft. **Yuqing Dong:** Supervision, Project administration. **Youxin Fang:** Supervision, Project administration. **Wei Gao:** Supervision, Project administration. **Xuemin Kang:** Investigation, Formal analysis. **Pengfei Liu:** Investigation, Data curation. **Shouxin Yan:** Formal analysis. **Bo Cui:** Conceptualization, Methodology, Writing - review & editing, Supervision. **A.M. Abd El-Aty:** Conceptualization, Methodology, Writing - review & editing, Supervision.

Declaration of Competing Interest

The authors declare that they have no known competing financial interests or personal relationships that could have appeared to influence the work reported in this paper.

Appendix A. Supplementary data

Supplementary data to this article can be found online at https://doi.org/10.1016/j.foodchem.2021.130804.

References

Arribas, C., Cabellos, B., Cuadrado, C., Guillamón, E., & Pedrosa, M. M. (2019). Extrusion effect on proximate composition, starch and dietary fibre of ready-to-eat products based on rice fortified with carob fruit and bean. *Lwt, 111*, 387–393. https://doi.org/10.1016/j.lwt.2019.05.064.

Bello-Pérez, L. A., Ottenhof, M. A., Agama-Acevedo, E., & Farhat, I. A. (2005). Effect of Storage Time on the Retrogradation of Banana Starch Extrudate. *Journal of Agricultural and Food Chemistry, 53*(4), 1081–1086. https://doi.org/10.1021/jf048858l.

BeMiller, J. N. (2011). Pasting, paste, and gel properties of starch–hydrocolloid combinations. *Carbohydrate Polymers, 86*(2), 386–423. https://doi.org/10.1016/j.carbpol.2011.05.064.

Cai, C., Wei, B., Tian, Y., Ma, R., Chen, L., Qiu, L., & Jin, Z. (2019). Structural changes of chemically modified rice starch by one-step reactive extrusion. *Food Chemistry, 288*, 354–360. https://doi.org/10.1016/j.foodchem.2019.03.017.

Capron, I., Robert, P., Colonna, P., Brogly, M., & Planchot, V. (2007). Starch in rubbery and glassy states by FTIR spectroscopy. *Carbohydrate Polymers, 68*(2), 249–259. https://doi.org/10.1016/j.carbpol.2006.12.015.

Chiu, C.-W., & Solarek, D. (2009). Chapter 17 - Modification of Starches. In J. BeMiller, & R. Whistler (Eds.), *Starch* (Third Edition, pp. 629–655). San Diego: Academic Press.

Dos Santos, T. P. R., Franco, C. M. L., Demiate, I. M., Li, X. H., Garcia, E. L., Jane, J. L., & Leonel, M. (2018). Spray-drying and extrusion processes: Effects on morphology and physicochemical characteristics of starches isolated from Peruvian carrot and cassava. *Int J Biol Macromol, 118*(Pt A), 1346–1353. https://doi.org/10.1016/j.ijbiomac.2018.06.070.

Fitch-Vargas, P. R., Aguilar-Palazuelos, E., de Jesus Zazueta-Morales, J., Vega-Garcia, M. O., Valdez-Morales, J. E., Martinez-Bustos, F., & Jacobo-Valenzuela, N. (2016). Physicochemical and Microstructural Characterization of Corn Starch Edible Films Obtained by a Combination of Extrusion Technology and Casting Technique. *J Food Sci, 81*(9), E2224–E2232. https://doi.org/10.1111/1750-3841.13416.

Garcia-Valle, Daniel E., Agama-Acevedo, Edith, Nuñez-Santiago, Maria del Carmen, Alvarez-Ramirez, José, & Bello-Pérez, Luis A. (2021). Extrusion pregelatinization improves texture, viscoelasticity and in vitro starch digestibility of mango and amaranth flours. *Journal of Functional Foods, 80*. https://doi.org/10.1016/j.jff.2021.104441.

Gomez, M. H., & Aguilera, J. M. (1984). A Physicochemical Model for Extrusion of Corn Starch. *Journal of Food Science, 49*(1), 40–43. https://doi.org/10.1111/j.1365-2621.1984.tb13664.x.

Gong, Bo, Cheng, Lilin, Gilbert, Robert G., & Li, Cheng (2019). Distribution of short to medium amylose chains are major controllers of in vitro digestion of retrograded rice starch. *Food Hydrocolloids, 96*, 634–643. https://doi.org/10.1016/j.foodhyd.2019.06.003.

Hu, Xiuting, Xu, Xueming, Jin, Zhengyu, Tian, Yaoqi, Bai, Yuxiang, & Xie, Zhengjun (2011). Retrogradation properties of rice starch gelatinized by heat and high hydrostatic pressure (HHP). *Journal of Food Engineering, 106*(3), 262–266. https://doi.org/10.1016/j.jfoodeng.2011.05.021.

Jiang, Qianqian, Xu, Xueming, Jin, Zhengyu, Tian, Yaoqi, Hu, Xiuting, & Bai, Yuxiang (2011). Physico-chemical properties of rice starch gels: Effect of different heat treatments. *Journal of Food Engineering, 107*(3), 353–357. https://doi.org/10.1016/j.jfoodeng.2011.07.006.

Koa, Su Sin, Jin, Xinglin, Zhang, Jing, & Sopade, Peter A. (2017). Extrusion of a model sorghum-barley blend: Starch digestibility and associated properties. *Journal of Cereal Science, 75*, 314–323. https://doi.org/10.1016/j.jcs.2017.04.007.

Li, C., & Gong, B. (2020). Insights into chain-length distributions of amylopectin and amylose molecules on the gelatinization property of rice starches. *Int J Biol Macromol, 155*, 721–729. https://doi.org/10.1016/j.ijbiomac.2020.04.006.

Li, Cheng, Wu, Alex, Yu, Wenwen, Hu, Yiming, Li, Enpeng, Zhang, Changquan, & Liu, Qiaoquan (2020). Parameterizing starch chain-length distributions for structure-property relations. *Carbohydr Polym, 241*, 116390. https://doi.org/10.1016/j.carbpol.2020.116390.

Li, Ming, Hasjim, Jovin, Xie, Fengwei, Halley, Peter J., & Gilbert, Robert G. (2014). Shear degradation of molecular, crystalline, and granular structures of starch during extrusion. 66(7-8), 595-605. 10.1002/star.201300201.

Liu, Cheng-mei, Liang, Rui-hong, Dai, Tao-tao, Ye, Jiang-ping, Zeng, Zi-cong, Luo, Shun-jing, & Chen, Jun (2016). Effect of dynamic high pressure microfluidization modified insoluble dietary fiber on gelatinization and rheology of rice starch. *Food Hydrocolloids, 57*, 55–61. https://doi.org/10.1016/j.foodhyd.2016.01.015.

Liu, Pengfei, Gao, Wei, Zhang, Xiaolei, Wu, Zhengzong, Yu, Bin, & Cui, Bo (2020). Physicochemical properties of pea starch-lauric acid complex modified by maltogenic amylase and pullulanase. *Carbohydr Polym, 242*, 116332. https://doi.org/10.1016/j.carbpol.2020.116332.

Liu, Pengfei, Gao, Wei, Zhang, Xiaolei, Wang, Bin, Zou, Feixue, Yu, Bin, … Cui, Bo (2021). Effects of ultrasonication on the properties of maize starch/stearic acid/sodium carboxymethyl cellulose composite film. *Ultrasonics Sonochemistry, 72*, 105447. https://doi.org/10.1016/j.ultsonch.2020.105447.

Liu, Y., Chen, J., Wu, J., Luo, S., Chen, R., Liu, C., & Gilbert, R. G. (2019). Modification of retrogradation property of rice starch by improved extrusion cooking technology. *Carbohydr Polym, 213*, 192–198. https://doi.org/10.1016/j.carbpol.2019.02.089.

Liu, Zhenyu, Wang, Chao, Liao, Xiaojun, & Shen, Qun (2020). Measurement and comparison of multi-scale structure in heat and pressure treated corn starch granule under the same degree of gelatinization. *Food Hydrocolloids, 108*, 106081. https://doi.org/10.1016/j.foodhyd.2020.106081.

Moad, Graeme (2011). Chemical modification of starch by reactive extrusion. *Progress in Polymer Science, 36*(2), 218–237. https://doi.org/10.1016/j.progpolymsci.2010.11.002.

Singh, Shivendra, Gamlath, Shirani, & Wakeling, Lara (2007). Nutritional aspects of food extrusion. *a review., 42*(8), 916–929. https://doi.org/10.1111/j.1365-2621.2006.01309.x.

Téllez-Morales, José A., Herman-Lara, Erasmo, Gómez-Aldapa, Carlos A., & Rodríguez-Miranda, Jesús (2020). Techno-functional properties of the starch-protein interaction during extrusion-cooking of a model system (corn starch and whey protein isolate). *Lwt, 132*, 109789. https://doi.org/10.1016/j.lwt.2020.109789.

van Soest, Jeroen J. G., Tournois, Hubertus, de Wit, Dick, & Vliegenthart, Johannes F. G. (1995). Short-range structure in (partially) crystalline potato starch determined with attenuated total reflectance Fourier-transform IR spectroscopy. *Carbohydrate Research, 279*, 201–214. https://doi.org/10.1016/0008-6215(95)00270-7.

von Borries-Medrano, Erich, Jaime-Fonseca, Mónica R., Aguilar-Méndez, Miguel A., & García-Cruz, Héctor I. (2018). Addition of galactomannans and citric acid in corn starch processed by extrusion: Retrogradation and resistant starch studies. *Food Hydrocolloids, 83*, 485–496. https://doi.org/10.1016/j.foodhyd.2018.03.009.

Wang, Bin, Yu, Bin, Yuan, Chao, Guo, Li, Liu, Pengfei, Gao, Wei, … Abd El-Aty, A. M. (2021). An overview on plasticized biodegradable corn starch-based films: The physicochemical properties and gelatinization process. *Critical Reviews in Food Science and Nutrition, 1–11*. https://doi.org/10.1080/10408398.2020.1868971.

Wang, Linfu, Shogren, Randal L., & Willett, Julious L. (1997). Preparation of Starch Succinates by Reactive Extrusion. *Starch - Stärke, 49*(3), 116–120. https://doi.org/10.1002/(ISSN)1521-379X10.1002/star.v49:310.1002/star.19970490308.

Wani, Idrees Ahmed, Farooq, Gousia, Qadir, Nafia, & Wani, Touseef Ahmad (2019). Physico-chemical and rheological properties of Bengal gram (Cicer arietinum L.) starch as affected by high temperature short time extrusion. *International Journal of Biological Macromolecules, 131*, 850–857. https://doi.org/10.1016/j.ijbiomac.2019.03.135.

Wu, A. C., Li, E., & Gilbert, R. G. (2014). Exploring extraction/dissolution procedures for analysis of starch chain-length distributions. *Carbohydr Polym, 114*(36–42), 4. https://doi.org/10.1016/j.carbpol.2014.08.001.

Xu, Xiaojuan, Chen, Yongzhi, Luo, Zhigang, & Lu, Xuanxuan (2019). Different variations in structures of A- and B-type starches subjected to microwave treatment and their relationships with digestibility. *Lwt, 99*, 179–187. https://doi.org/10.1016/j.lwt.2018.09.072.

Yan, Xiang, Wu, Zheng-Zong, Li, Ming-Yang, Yin, Fei, Ren, Ke-Xin, & Tao, Han (2019). The combined effects of extrusion and heat-moisture treatment on the physicochemical properties and digestibility of corn starch. *International Journal of Biological Macromolecules, 134*, 1108–1112. https://doi.org/10.1016/j.ijbiomac.2019.05.112.

Yin, Xiuxiu, Ma, Zhen, Hu, Xinzhong, Li, Xiaoping, & Boye, Joyce I. (2018). Molecular rearrangement of Laird lentil (Lens culinaris Medikus) starch during different processing treatments of the seeds. *Food Hydrocolloids, 79*, 399–408. https://doi.org/10.1016/j.foodhyd.2018.01.012.

Yu, Chen, Liu, Junfei, Tang, Xiaozhi, Shen, Xinchun, & Liu, Shaowei (2017). Correlations between the physical properties and chemical bonds of extruded corn starch enriched with whey protein concentrate. *RSC Advances, 7*(20), 11979–11986. https://doi.org/10.1039/C6RA26764E.

Yu, Shifeng, Ma, Ying, & Sun, Da-Wen (2009). Impact of amylose content on starch retrogradation and texture of cooked milled rice during storage. *Journal of Cereal Science, 50*(2), 139–144. https://doi.org/10.1016/j.jcs.2009.04.003.

Zaidul, I. S. M., Norulaini, N. A., Nik, Omar, Mohd, A. K., Yamauchi, H., & Noda, T. (2007). RVA analysis of mixtures of wheat flour and potato, sweet potato, yam, and cassava starches. *Carbohydrate Polymers, 69*(4), 784–791. https://doi.org/10.1016/j.carbpol.2007.02.021.

Zhang, Gaopeng, Ni, Chunlei, Ding, Yangyue, Zhou, Hualu, Caizhi, Ou, Wang, Qiuye, … Cheng, Jianjun (2020). Effects of Low Moisture Extrusion on the Structural and Physicochemical Properties of Adlay (Coix lacryma-jobi L.) Starch-Based Polymers. *Process Biochemistry, 96*, 30–37. https://doi.org/10.1016/j.procbio.2020.05.028.

Zhang, Yanjun, Hu, Meijie, Zhu, Kexue, Wu, Gang, & Tan, Lehe (2018). Functional properties and utilization of Artocarpus heterophyllus Lam seed starch from new species in China. *International Journal of Biological Macromolecules, 107*, 1395–1405. https://doi.org/10.1016/j.ijbiomac.2017.10.001.